Journal of Power Sources 195 (2010) 1845–1848

Contents lists available at ScienceDirect

Journal of Power Sources

journal homepage: www.elsevier.com/locate/jpowsour

Short communication

High-performance anode-supported Solid Oxide Fuel Cells based on $Ba(Zr_{0.1}Ce_{0.7}Y_{0.2})O_{3-\delta}$ (BZCY) fabricated by a modified co-pressing process

Lei Yang*, Chendong Zuo[1], Meilin Liu[1]

School of Materials Science and Engineering, Georgia Institute of Technology, 771 Ferst Drive, Atlanta, GA 30332-0245, USA

ARTICLE INFO

Article history:
Received 10 September 2009
Received in revised form 6 October 2009
Accepted 7 October 2009
Available online 17 October 2009

Keywords:
BZCY
Anode-supported
Modified co-pressing
Conductivity

ABSTRACT

A modified co-pressing process was developed to fabricate anode-supported dense and uniform $Ba(Zr_{0.1}Ce_{0.7}Y_{0.2})O_{3-\delta}$ (BZCY) electrolyte films (~20 μm thick) from BZCY powders with different characteristics; the powders derived from a glycine nitrate process was used for the anode whereas the powders from solid state reaction for the electrolyte. The BZCY electrolyte films sintered at 1350 °C for 6 h reached a conductivity of ~0.025 S cm^{-1} at 700 °C, similar to that of BZCY pellet sintered at 1550 °C for 10 h. Further, a test cell based on such an anode-supported BZCY electrolyte demonstrated peak power densities of ~780 and ~490 mW cm^{-2} at 700 and 600 °C, respectively.

1. Introduction

Oxide proton conductors are promising electrolytes for low-temperature SOFCs because of their relatively high ionic conductivities at low temperatures [1–8]. To date, electrolyte-supported cells were commonly used due to difficulties associated with fabrication of anode-supported cells, leading to much lower performance in comparison to anode-supported cells using yttria-stabilized zirconia (YSZ) or gadolinia doped ceria (GDC) as the electrolyte [1,9]. For example, isostatic pressing at 216 MPa followed by sintering at 1600 °C for 10 h was required to form dense $BaCe_{0.8}Gd_{0.2}O_{3-d}$ pellets of ~1 mm thick [10]. These electrolyte-supported cells with $La_{0.6}Sr_{0.4}CoO_{3-\delta}$ cathodes demonstrated a peak power density of ~5.5 mW cm^{-2} at 700 °C under typical fuel cell operating conditions.

A reactive sintering process was recently developed for fabrication of thin and dense proton conducting electrolyte films on Ni-based anodes at relatively low temperatures (~1400 °C) [11–14]. The reactions among precursors ($BaCO_3$, CeO_2, and Y_2O_3) in the anode and electrolyte layers facilitated densification of the electrolyte films. However, it is noted that the conductivities of these electrolyte films are far lower than the anticipated values. For example, a 25 μm thick $Ba(Zr_{0.1}Ce_{0.7}Y_{0.2})O_{3-\delta}$ (BZCY) electrolyte showed an area-specific Ohmic resistance of ~0.5 Ω cm^2 at 700 °C [12], corresponding to conductivity of 0.005 S cm^{-1}; however, the conductivity of a properly sintered BZCY pellet at 700 °C should be ~0.021 S cm^{-1} [4]. The large discrepancy in conductivity is due probably to the non-stoichiometry in BZCY resulting from complicated synthesis reactions at 1400 °C, especially Ba evaporation from carbonate during sintering [15,16]. It was reported that $BaCO_3$ experienced maximum mass loss at ~1200 °C and the resultant BaO is extremely volatile at this temperature [17]. In contrast, the Ba loss in $BaCeO_3$ is relatively small even at ~1500 °C [13]. Electrical conductivity of cerates and zirconates depends sensitively on stoichiometry; small deviation from desired composition might dramatically reduce conductivity, sinterability, and chemical stability in atmospheres containing H_2O and CO_2 [18,19]. Therefore, it is necessary to develop a process for fabrication of BZCY films supported by anode while maintaining the desired compositions and properties.

In this communication, we report a modified co-pressing, co-firing process for fabrication of anode-supported BZCY electrolyte films with high electrical conductivity (~0.025 S cm^{-1} at 700 °C) at relatively low sintering temperature (1350 °C for 6 h) using BZCY powders derived from a glycine nitrate process for the anode whereas the powders from solid state reaction for the electrolyte. This unique fabrication process produced uniform, homogeneous, and dense BZCY films of ~20 μm supported by anode; single cells based on these anode-supported BZCY films demonstrated much higher power densities.

2. Experimental

Two different methods were used to prepare $Ba(Zr_{0.1}Ce_{0.7}Y_{0.2})O_{3-\delta}$ powders. In the solid state reaction (SSR) method, stoichiometric amounts of high-purity barium carbonate,

* Corresponding author. Tel.: +1 404 894 6114; fax: +1 404 894 9140.
E-mail addresses: lyang7@gatech.edu (L. Yang), meilin.liu@mse.gatech.edu (M. Liu).
[1] Tel.: +1 404 894 6114; fax: +1 404 894 9140.

0378-7753/$ – see front matter © 2009 Elsevier B.V. All rights reserved.
doi:10.1016/j.jpowsour.2009.10.018

zirconium oxide, cerium oxide, and yttrium oxide powders (all from Aldrich Chemicals) were mixed using ball milling with stabilized zirconia media in ethanol for 48 h. The resultant mixture was dried at 60 °C for 24 h, followed by calcination at 1100 °C for 10 h. The ball milling and calcination under same conditions were repeated twice to obtain pure phase. In the glycine nitrate process (GNP), suitable amounts of $Ba(NO_3)_2$, $Ce(NO_3)_3$, $Y(NO_3)_3$, and $ZrO(NO_3)_2$ (all from Aldrich Chemicals) were dissolved in distilled water (0.1 M) and mixed with glycine (molar ratio of NO_3^- to glycine = 1.5:1). Then the solution was heated on a hot plate to vaporize water, converted to gel, and finally ignited to flame. The resultant yellow ash was then fired at 900 °C for 2 h to obtain BZCY powders. In subsequent discussions, BZCY–SSR stands for BZCY powders prepared by a solid state reaction process whereas BZCY–GNP for those derived from a glycine nitrate process.

A co-pressing and co-firing process was then used to prepare anode-supported electrolyte bilayers. Mixed powders of NiO, BZCY–GNP, and rice starch (from Aldrich Chemicals) with a weight ratio of 65:35:10 was pre-pressed at 100 MPa in a stainless steel mold as the substrate. Subsequently the BZCY powders from SSR were added to the surface of green anode through a screen (500 meshes) to guide uniform distribution of BZCY powders on the anode. Without a screen, it is difficult to uniformly and fully cover the anode when the amount of BZCY electrolyte powders was relatively small to make the electrolyte layer sufficiently thin. The anode-supported electrolyte bilayers were uniaxially co-pressed at 250 MPa, followed by sintering at 1350 °C for 6 h.

Composite cathode consisting of $Sm_{0.5}Sr_{0.5}CoO_{3-\delta}$ (SSC, derived from GNP as describe elsewhere [3]) and BZCY (weight ratio of 7:3) were prepared as follows. The mixture of SSC and BZCY was mixed with V006 and acetone (weight ratio of 1:1:1) to form a cathode slurry, which was brush-painted on the BZCY electrolyte. The composite cathode was then fired at 1000 °C for 3 h. All the cells in this report utilized same cathode; the only difference is the various combinations of BZCY powders in anode and electrolyte. For simplicity, cells were labeled with the process method used for fabrication of the BZCY powders. For example, GNP/SSR denotes the cell that used BZCY powder derived from GNP for the anode and BZCY powder from SSR for the electrolyte.

The phase of BZCY was examined by XRD (PW-1800 system, 2θ = 20–80°). The morphologies of the cell components were observed using a Hitachi S-800 scanning electron microscope. All standard electrochemical experiments were performed using a Solartron 1286 electrochemical interface and a Solartron 1255 HF frequency response analyzer.

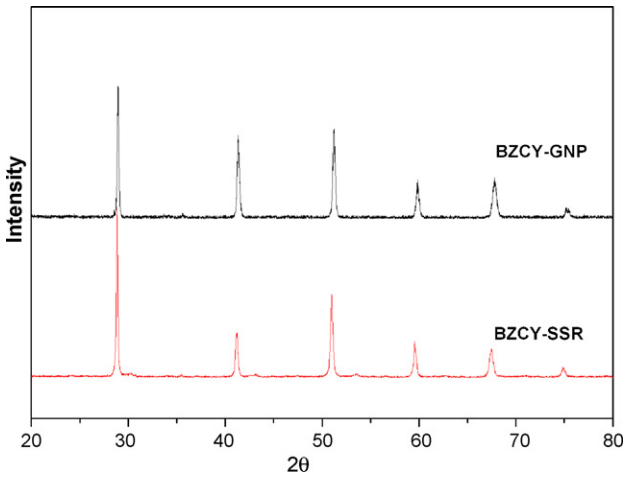

Fig. 1. X-ray diffraction patterns of the BZCY powder synthesized by glycine nitrate process and solid state reaction.

3. Results and discussion

Fig. 1 shows typical X-ray diffraction patterns of the BZCY powders prepared by solid state reaction and glycine nitrate process, suggesting that single phase was obtained using both methods. This is required to ensure high conductivity and stability. Shown in Fig. 2 are the typical morphologies of BZCY powders by the two methods. The BZCY powder prepared by the SSR process has relatively high filling density; each individual particle is relatively dense and dry pressing of the powder may result in high packing density of green body. In contrast, the BZCY powder derived from a GNP process are highly porous; the pore sizes ranged from tens of nanometers to sub-micrometers. The low filling density of the GNP powders would result in large amount of shrinkage during firing. When used in the anode support, the BZCY powder derived from a GNP process would lead to accelerated densification of the electrolyte during firing; it may help to increase triple phase boundary length of the anode as well.

Other combinations of BZCY powders were also examined under identical co-pressing and co-firing conditions. Fig. 3(a) shows the cross-sectional morphology of a cell using BZCY–SSR powders in both anode and electrolyte. Obviously, some pinholes were observable in the BZCY electrolyte, due primarily to insufficient shrinkage (~12% in diameter) after sintering. Higher sintering temperature will yield denser electrolyte, but may cause deactivation of the anode. Fig. 3(b) shows the microstructures of an anode-

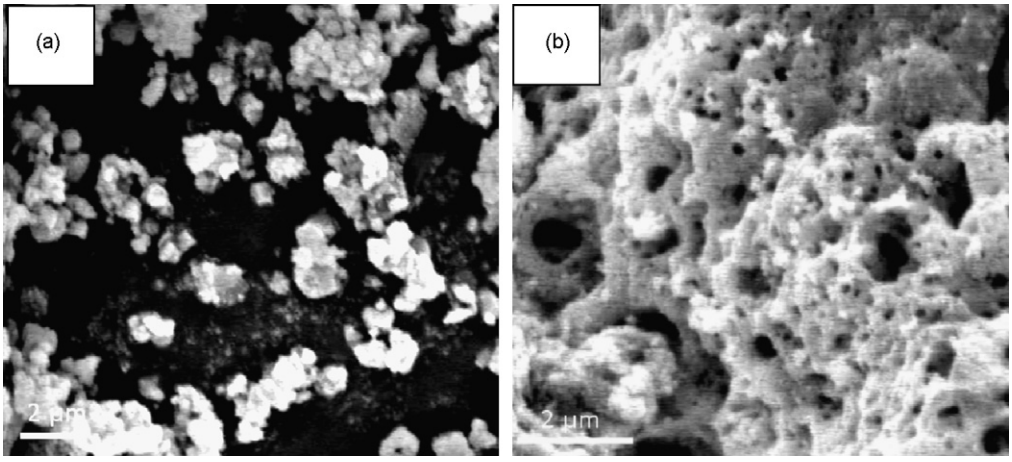

Fig. 2. Morphologies of BZCY powders prepared by (a) a solid state reaction and (b) a glycine nitrate process.

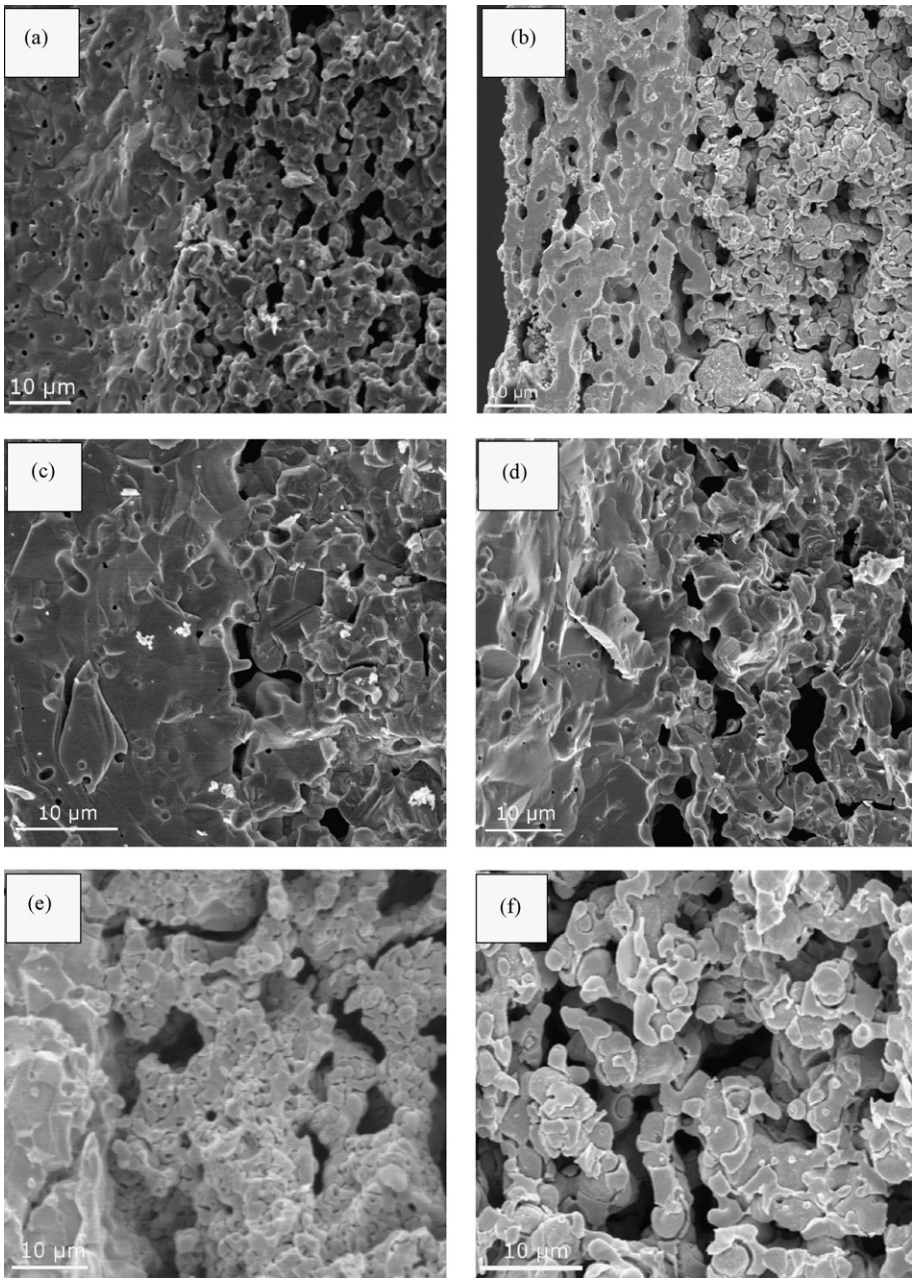

Fig. 3. Cross-sectional views of anode/electrolyte bilayers. (I) Before reduction: (a) SSR/SSR, (b) GNP/GNP, (c) GNP/SSR with 10 wt% starch and (d) GNP/SSR with 20 wt% starch. (II) After reduction: (e) GNP/SSR with 20 wt% starch and (f) GNP/SSR with 10 wt% starch. The left and right layers are electrolyte and anode, respectively.

supported electrolyte bilayers using only the BZCY powder derived from GNP. It is seen that the electrolyte film was still porous and remained almost the same even after the sintering temperature was increased to 1400 °C. Although large surface areas of powders provide increased driving force for densifications, high packing density of green pellet is also essential to decreasing the porosity of sintered body. The foam structure of BZCY–GNP is probably difficult to eliminate closed pores. In contrast, when the BZCY powder derived from GNP was used for the Ni–BZCY anode while that from SSR for the BZCY electrolyte, the electrolyte film is very dense and well-adhered to the porous anode substrate. The use of foam BZCY powder derived from GNP in the anode greatly facilitated the sintering of the electrolyte layer, reaching a linear shrinkage of ~18%.

When powders derived form a GNP process is used for dry pressing of the electrolyte film, it is relatively easy to form a uniform electrolyte layer because of the relatively low filling density of GNP powders (or large volume of the powder). Since the filling density of the BZCY powder prepared by a SSR process is relatively high, however, the volume of the powder for a 20 μm thick electrolyte film is very small, making it very difficult to uniformly distribute the powder on the green anode substrate. As a result, variation in thickness of the BZCY layer is relatively large. In some areas, the electrolyte is so thin to result in short circuiting of the cell. To overcome this difficulty, we used a screen to carefully improve the uniformity of the SSR powder distribution onto the anode substrate. This modified co-pressing allows us to fabricate crack-free films with ~20 μm of thickness even from commercially available powders with relatively large particle size, as shown in Fig. 3(c).

In addition to achieving uniform and dense BZCY electrolyte film, optimization of the anode microstructure is also important

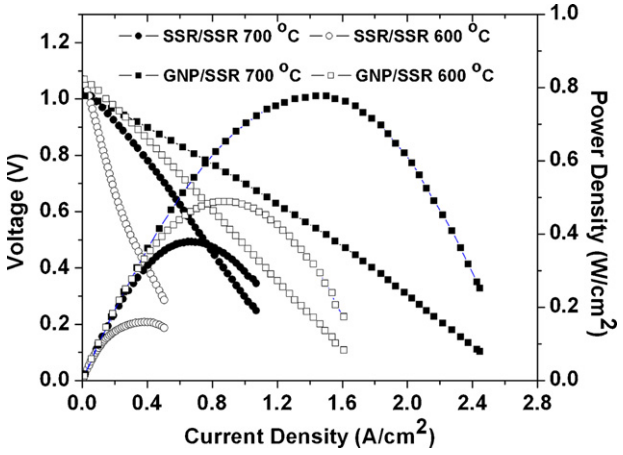

Fig. 4. Terminal voltage and power density as a function of current density for GNP/SSR and SSR/SSR cells when ambient air was used as oxidant and hydrogen (with ~3 vol.% H_2O) as fuel. Cathode is BZCY–SSC composite.

to enhancing fuel cell performance. For example, pore formers are often added in anode processing to create path of gas transport. Fig. 3(c) and (d) compares the morphologies of two cells using 10 and 20 wt% starch (pore former) in the NiO–BZCY anode. The anode with 20 wt% starch shows slightly higher porosity. After reduction in H_2, however, cracks were formed near the interface in addition to numerous inhomogeneous pores, as shown in Fig. 3(e). These are due probably to the large and non-uniform shrinkage of anode. In contrast, the sample with 10 wt% starch in the anode showed a more uniform microstructure, better connectivity, and stronger bonding between the anodes and the electrolyte bilayers (Fig. 3(f)).

Fig. 4 shows the current–voltage characteristics and the corresponding power densities for 2 cells prepared by the co-pressing and co-firing process using BZCY electrolyte powders derived from two different processes: SSR/SSR and GNP/SSR cells with BZCY electrolyte film of ~20 μm thick. The open circuit voltages (OCV) of the two cells are similar (both above 1.0 V), an indication of sufficiently dense electrolytes. However, much higher peak power densities was observed for the GNP/SSR cell, reaching 780 and 490 mW cm^{-2} at 700 and 600 °C, respectively. The SSR/SSR cell produced only ~379 and 160 mW cm^{-2} under the same testing conditions. The relatively poor performance of the SSR/SSR cell is attributed to the large amount of closed pores in the electrolyte, which significantly reduced the conductivity of the electrolyte. The undesired microstructure also resulted in higher electrode polarization resistances because of the sluggish transfer of ions across the electrode/electrolyte interface.

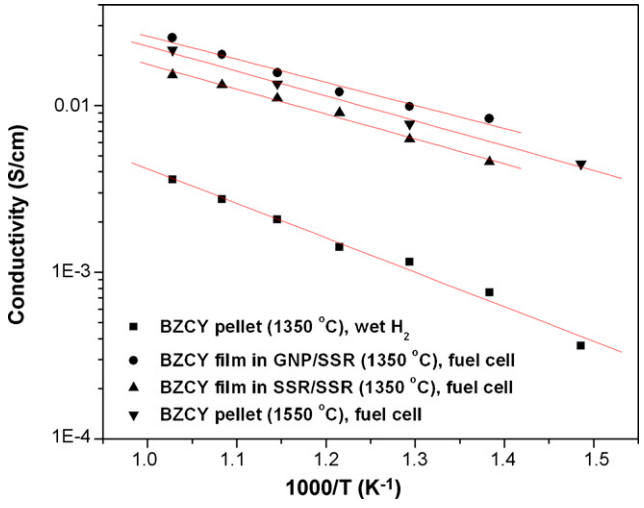

Fig. 5. Conductivities of BZCY pellets sintered at 1550 and 1350 °C for 10 h and the BZCY electrolyte films in a SSR/SSR and a GNP/SSR cell fired at 1350 °C for 6 h.

Fig. 5 shows the conductivities of BZCY pellets and anode-supported BZCY films measured in wet H_2 and under fuel cell operation conditions. The BZCY pellets were sintered at 1350 and 1550 °C for 10 h, whereas the BZCY electrolyte films in SSR/SSR and GNP/SSR cells were fired at 1350 °C for 6 h. Obviously, the BZCY electrolyte film in a GNP/SSR cell exhibited a conductivity of 0.025 S cm^{-1} at 700 °C, much greater than the conductivities of the BZCY electrolyte film in a SSR/SSR cell or the BZCY pellets fired at 1350 °C for 10 h. These large differences in conductivity are attributed to the high porosity of the electrolyte samples. The conductivity of the BZCY film in the SSR/GNP cell is comparable to those of the BZCY pellets fired at 1550 °C for 10 h, suggesting that the anode substrate containing foam BZCY powder derived from GNP dramatically reduced the sintering temperature of BZCY electrolyte containing SSR powders.

4. Conclusions

The present study demonstrated that a dense and uniform BZCY electrolyte film (~20 μm) was fabricated on a porous anode support at a relatively low temperature by a modified co-pressing, co-firing process using BZCY powders with different characteristics. The conductivities of the BZCY electrolyte film in an anode-supported cell (fired at 1350 °C for 6 h) are comparable to those of BZCY pellets (sintered at 1550 °C for 10 h). Single cells based on anode-supported BZCY electrolyte films demonstrated much-improved power output, achieving peak power densities of ~780 and ~490 mW cm^{-2} at 700 and 600 °C, respectively.

Acknowledgement

This work was supported by U.S. Department of Energy, Office of Basic Energy Sciences, grant DE-FG02-06ER15837.

References

[1] K.D. Kreuer, Annual Review of Materials Research 33 (2003) 333–359.
[2] J.H. Shim, T.M. Gur, F.B. Prinz, Applied Physics Letters 92 (2008).
[3] L. Yang, C.D. Zuo, S.Z. Wang, Z. Cheng, M.L. Liu, Advanced Materials 20 (2008) 3280–3283.
[4] C.D. Zuo, S.W. Zha, M.L. Liu, M. Hatano, M. Uchiyama, Advanced Materials 18 (2006) 3318–3320.
[5] L. Yang, Z. Liu, S. Wang, Y. Choi, C.D. Zuo, M.L. Liu, Journal of Power Sources 195 (2010) 471–474.
[6] T. Norby, Solid State Ionics 125 (1999) 1–11.
[7] V. Agarwal, M.L. Liu, Journal of the Electrochemical Society 144 (1997) 1035–1040.
[8] J. Guan, S.E. Dorris, U. Balachandran, M. Liu, Solid State Ionics 100 (1997) 45–52.
[9] T. Hibino, A. Hashimoto, M. Suzuki, M. Sano, Journal of the Electrochemical Society 149 (2002) A1503–A1508.
[10] N. Maffei, L. Pelletier, A. McFarlan, Journal of Power Sources 136 (2004) 24–29.
[11] L. Bi, S.Q. Zhang, S.M. Fang, L. Zhang, K. Xie, C.R. Xia, W. Liu, Electrochemistry Communications 10 (2008) 1005–1007.
[12] B. Lin, Y.C. Dong, R.Q. Yan, S.Q. Zhang, M.J. Hu, Y. Zhou, G.Y. Meng, Journal of Power Sources 186 (2009) 446–449.
[13] J.M. Serra, W.A. Meulenberg, Journal of the American Ceramic Society 90 (2007) 2082–2089.
[14] J.M. Serra, O. Buchler, W.A. Meulenberg, H.P. Buchkremer, Journal of the Electrochemical Society 154 (2007) B334–B340.
[15] S. Barison, M. Battagliarin, T. Cavallin, S. Daolio, L. Doubova, M. Fabrizio, C. Mortalo, S. Boldrini, R. Gerbasi, Fuel Cells 8 (2008) 360–368.
[16] Y. Yamazaki, R. Hernandez-Sanchez, S.M. Haile, Chemistry of Materials 21 (2009) 2755–2762.
[17] D. Hirabayashi, A. Tomita, S. Teranishi, T. Hibino, M. Sano, Solid State Ionics 176 (2005) 881–887.
[18] S.M. Haile, G. Staneff, K.H. Ryu, Journal of Materials Science 36 (2001) 1149–1160.
[19] F. Iguchi, T. Tsurui, N. Sata, Y. Nagao, H. Yugami, Solid State Ionics 180 (2009) 563–568.